Jerzy GOŁĘBIOWSKI, Marek ZARĘBA

Bialystok Technical University, Faculty of Electrical Engineering, Department of Theoretical Electrotechnics and Metrology

doi:10.15199/48.2015.10.56

Plano-parallel models of the electrical systems with non-uniform heat exchange on a perimeter Part I. Stationary thermal field

Abstract. *The stationary thermal field in a plano-parallel system was determined in the article with the aid of an analytical method. Three different coefficients of the heat transfer were assumed on a perimeter of the system cross-section. The temperature distribution was obtained by superposition of the particular integral of Poisson's equation and a general integral of Laplace's equation, taking into account Hankel's boundary conditions. The problem considered here can be a mathematical model of the two-dimensional thermal field in a rectangular DC busway or in a long dielectric capacitative heated. For this reason the method of determination of the steady state current rating and the maximal electric field strength in a dielectric was presented in the paper. The results of computations were numerically verified and presented in the graphic form.*

Streszczenie. *Za pomocą metody analitycznej w artykule wyznaczono stacjonarne pole termiczne w płasko-równoległym układzie. Na obwodzie jego przekroju założono trzy różne współczynniki przejmowania ciepła. Rozkład temperatury uzyskano superponując całkę szczególną równania Poissona i ogólną równania Lapalce'a z uwzględnieniem warunków brzegowych Hankela. Rozpatrywane zagadnienie może stanowić model matematyczny dwuwymiarowego pola termicznego w prostokątnym szynoprzewodzie DC lub w długim dielektryku nagrzewanym pojemnościowo. Z tego powodu w pracy przedstawiono metodę wyznaczania długotrwałego prądu dopuszczalnego i maksymalnego natężenia pola elektrycznego w dielektryku. Wyniki zweryfikowano na drodze numerycznej i przedstawiono w postaci graficznej.(**Płasko-równoległe modele układów elektrycznych z nierównomiernym oddawaniem ciepła na obwodzie. Część I. Stacjonarne pole temperatury**)*

Keywords:, analytical methods of the field theory, stationary thermal field, computer aid, steady state current rating
Słowa kluczowe: analityczne metody teorii pola, stacjonarne pole termiczne, wspomaganie komputerowe, długotrwały prąd dopuszczalny

Introduction

Plano-parallel thermal models are the systems, which length is significantly larger than their cross-sectional dimensions. Moreover, the field sources and boundary conditions should be constant along the length of a model. The examples of the mentioned systems are: long sections of a DC busway with the rectangular cross-section and cubicoidal dielectric charges placed in the electrode heaters (e.g. in wood drying and laminates manufacturing). In the first case an uniform distribution of the heating power density is obvious (lack of the skin effect). In turn capacitative heating the analogical effect is observed for a zero potential of one of the electrodes of a heating capacitor and a small difference of the potentials on the other one (10% maximum). In practice it is realized by supplying the heating capacitor at many points or by the respective connection of an inductance between electrodes [1]. The other method of equalization of the electric field in a charge is reduction of a frequency of the capacitor supply source.

In case of the rectangular DC busway a knowledge of the temperature distribution in the steady state is very useful for an accurate determination of the steady state current rating [2], [3]. In turn in the capacitative heating a stationary distribution of the temperature has a great importance in the sustained heat generation by a small power [4]. Then it is also important to determine the warmest point of a charge, what prevents, among others, a loss of its desirable properties or even a devastation. Also a difference between the maximal and minimal temperature (i.e. gradient) is important.

The stationary thermal field can be determined by the analytical and numerical way, as well. Basic advantage of the analytical solution are the results in the form of formulas. They enable, among others, discussion on the influence of particular parameters and physical interpretation of the obtained results, as well. Besides formulas enable to test the programs for numerical computations. From the above presented reasons the authors decided for an analytical solution of the problem.

In [5], [6], [7] the thermal field of a plano-parallel model was determined in terms of the convectional heat exchange. The heat transfer coefficient was assumed identical on the whole perimeter of the system. In [5] the thermal field of a column of the transformer was analyzed, where two different heat transfer coefficients were assumed (but the same on opposite surfaces of the system). The above mentioned problems were solved in [5], [6], [7] by the Roth method (i.e. by eigenfunctions of the Laplace's operator [8]) and by the method of integral transformations [9]. In the present paper the separation of variables method [10] was applied instead. Such an approach is motivated by more simple and more convenient final solution in the form of single series (in [5], [6], [7] double series were obtained of much worse convergence). The selected method enabled to avoid troubles connected with realization of the inverse integral transformation [9]. In authors opinion an original element of the presented article is consideration on the analytical way of three different heat transfer coefficients on a perimeter of the system (Fig. 1, $\alpha_H \neq \alpha_L \neq \alpha_V$). Such a model better responds to the real heat exchange than the one with a constant value of the coefficient on the whole edge of the system [5], [6], [7].

Boundary problem of the plano-parallel field model

The subject of the analysis is a plano-parallel system, which cross-section is shown in Fig. 1. It is convenient to present the boundary problem with respect to a thermal increment $v_s(x,y)$, referred to the ambient temperature T_o

$$v_s(x,y) = T_s(x,y) - T_o \,, \tag{1}$$

where: $T_s(x,y)$, - stationary temperature field distribution in the system.

Temperature increase (1) with the assumption of a homogeneous structure of the model material is described by the Poisson equation [11], [12]

$$\frac{\partial^2 v_s(x,y)}{\partial x^2} + \frac{\partial^2 v_s(x,y)}{\partial y^2} = -\frac{g}{\lambda} \quad \text{for} \quad |x| \le a \quad \text{and} \tag{2}$$

$0 \le y \le b$, where:

(2a) $g = \frac{\rho I^2}{4a^2 b^2}$ - efficiency of spatial heat sources in case of a DC busway or

(2b) $g = \omega \varepsilon' (tg\delta) E^2$ - efficiency of spatial heat sources in case of a dielectric charge [1], λ - specific thermal conductivity, ρ - specific resistivity, I - DC current intensity, *(2a,b)* – cross-sectional dimensions of the system (Fig. 1), ω - supplying pulsation, ε' - real part of the complex permittivity of a charge, $tg\delta$ - loss coefficient, E - rms value of the electric field.

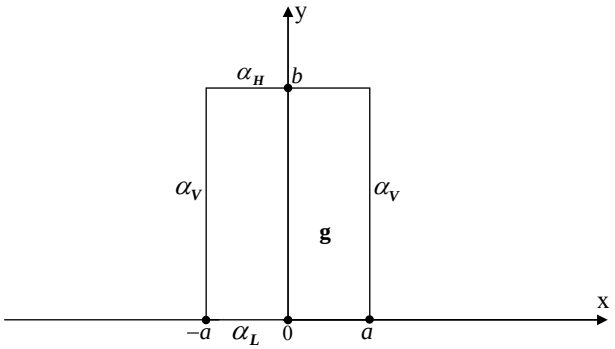

Fig. 1. Cross section of the plano-parallel model

In the model discussed it was assumed, that the heat exchange with surroundings takes place according with Newton's rule [12] with different heat transfer coefficients on a perimeter of the system. Opposite vertical walls of the model (Fig. 1, $x=\pm a$) give up the heat identically with the same coefficient α_V. Then there is a symmetry of the field distribution with respect to the plane $x=0$. The above conclusions were described by the following boundary conditions

(3a) $$\left.\frac{\partial v_s(x,y)}{\partial x}\right|_{x=a} = -\frac{\alpha_V}{\lambda} v_s(x=a,y),$$

(3b) $$\left.\frac{\partial v_s(x,y)}{\partial x}\right|_{x=0} = 0.$$

In turn the heat exchange on the bottom and on the top horizontal edges takes place with different coefficients (respectively α_L for $y=0$ and α_H for $y=b$, Fig. 1). It is described by the following boundary conditions

(3c) $$\left.\frac{\partial v_s(x,y)}{\partial y}\right|_{y=0} = \frac{\alpha_L}{\lambda} v_s(x,y=0),$$

(3d) $$\left.\frac{\partial v_s(x,y)}{\partial y}\right|_{y=b} = -\frac{\alpha_H}{\lambda} v_s(x,y=b).$$

In equations (3a,c,d) the total coefficients of the heat transfer were appeared. It means, that they consider the convection and radiation, as well.

Equations (1)-(3) form the boundary problem of the investigated stationary field.

Solution of the boundary problem of the model

The solution of (2) is a superposition of integrals: the particular one of the heterogeneous equation (Poisson's) and a general one of the homogeneous equation (Laplace's) [13]. Because the function (field source) on the right side of (2) is constant, the particular integral was anticipated in the form of the second degree polynomial. The general integral was determined by separation of variables [10] in Laplace's equation (i.e. with the zeroed right side of (2)) with the constant $(\gamma_n/b)^2$. After consideration of the thermal conditions symmetry with respect to the plane $x=0$ (i.e. evenness of the solution) it was obtained finally, that

(4) $$v_s(x,y) = -\frac{gy^2}{2\lambda} + Ay + B + \sum_{n=1}^{\infty} \cosh(\gamma_n \frac{x}{b}) \left[C_n \sin(\gamma_n \frac{y}{b}) + D_n \cos(\gamma_n \frac{y}{b}) \right]$$

for $|x| \le a$ and $0 \le y \le b$, where: A,B - constants, C_n,D_n - coefficients of trigonometric series, γ_n - dimensionless eigenvalues of the problem. Relation (4) fulfils equation (3b). With the aid of (3c) and (4) the number of constants and coefficients of the series were reduced. Relation (4) takes then the form of

(5a) $$v_s(x,y) = -\frac{gy^2}{2\lambda} + B\frac{\alpha_L}{\lambda} y + B + \sum_{n=1}^{\infty} D_n \cosh(\gamma_n \frac{x}{b}) \left[\frac{\alpha_L b}{\gamma_n \lambda} \sin(\gamma_n \frac{y}{b}) + \cos(\gamma_n \frac{y}{b}) \right]$$

Introducing (5a) to (3d) a constant was determined

(5b) $$B = \frac{2bg\lambda + b^2 g \alpha_H}{2(\lambda\alpha_L + \lambda\alpha_H + b\alpha_L\alpha_H)}$$

and the equation of eigenvalues

(6) $$tg\gamma_n = \frac{(\alpha_L + \alpha_H) b \gamma_n \lambda}{\gamma_n^2 \lambda^2 - \alpha_L \alpha_H b^2},$$

where γ_n are consecutive positive roots of equation (6).

It is necessary to determine the unknown coefficient D_n in (5a), as well. For this reason (5a) was introduced to (3a)

(7) $$\sum_{n=1}^{\infty} D_n \left(\frac{\gamma_n}{b} \sinh(\gamma_n \frac{a}{b}) + \frac{\alpha_V}{\lambda} \cosh(\gamma_n \frac{a}{b}) \right) \left(\frac{\alpha_L b}{\gamma_n \lambda} \sin(\gamma_n \frac{y}{b}) + \cos(\gamma_n \frac{y}{b}) \right) = -\frac{\alpha_V}{\lambda} \left(-\frac{gy^2}{2\lambda} + B\frac{\alpha_L}{\lambda} y + B \right).$$

Then relation (7) was multiplied by $\left\{ \frac{\alpha_L b}{\gamma_m \lambda} \sin(\gamma_m \frac{y}{b}) + \cos(\gamma_m \frac{y}{b}) \right\}$ and integrated by sides with respect to the coordinate y in a sector $\langle 0,b \rangle$. Orthogonality of the given above sequence of functions $\{\ldots\}$ in the considered sector was used (respective proof is presented in the appendix). Finally coefficient D_m is expressed as below

(8) $$D_m = \frac{\int_0^b \left(\frac{gy^2\alpha_V}{2\lambda^2} - \frac{\alpha_V\alpha_L}{\lambda^2} By - \frac{\alpha_V}{\lambda} B \right) \left(\frac{\alpha_L b}{\gamma_m \lambda} \sin(\gamma_m \frac{y}{b}) + \cos(\gamma_m \frac{y}{b}) \right) dy}{\left(\frac{\alpha_V}{\lambda} \cosh(\gamma_m \frac{a}{b}) + \frac{\gamma_m}{b} \sinh(\gamma_m \frac{a}{b}) \right) \cdot \|N(m)\|^2},$$

where: B is given by formula (5b) and

$\|N(m)\|^2 = \int_0^b \left(\frac{\alpha_L b}{\gamma_m \lambda} \sin(\gamma_m \frac{y}{b}) + \cos(\gamma_m \frac{y}{b}) \right)^2 dy$ - is a square of the norm [12] of the functional sequence given in the above.

After computation of the respective integrals in (8), taking advantage of the equation of eigenvalues (6) and simplifications, the investigated coefficient D_m was expressed by the formula

(9) $$D_m = \frac{-2g\alpha_V b^4\left[\gamma_m\lambda\alpha_L b(\alpha_L+\alpha_H)+\alpha_H\left(\gamma_m^2\lambda^2+b^2\alpha_L^2\right)\sin(\gamma_m)\right]}{\gamma_m\left(\alpha_L^2b^2+\gamma_m^2\lambda^2\right)\left[\gamma_m^2\lambda b(\alpha_L+\alpha_H)+\left(\gamma_m^2\lambda^2+b^2\alpha_L\alpha_H\right)\sin^2(\gamma_m)\right]\left(\alpha_V b\cosh(\gamma_m\frac{a}{b})+\gamma_m\lambda\sinh(\gamma_m\frac{a}{b})\right)}.$$

Finally the stationary temperature distribution in the system results from relation (1)

(10) $$T_s(x,y) = T_o + v_s(x,y),$$

where: increase $v_s(x,y)$ is given by formula (5a), coefficient D_n was determined with the aid of (9) (after exchange $m \rightarrow n$), where constant B and eigenvalues γ_n were determined from (5b) and (6), respectively.

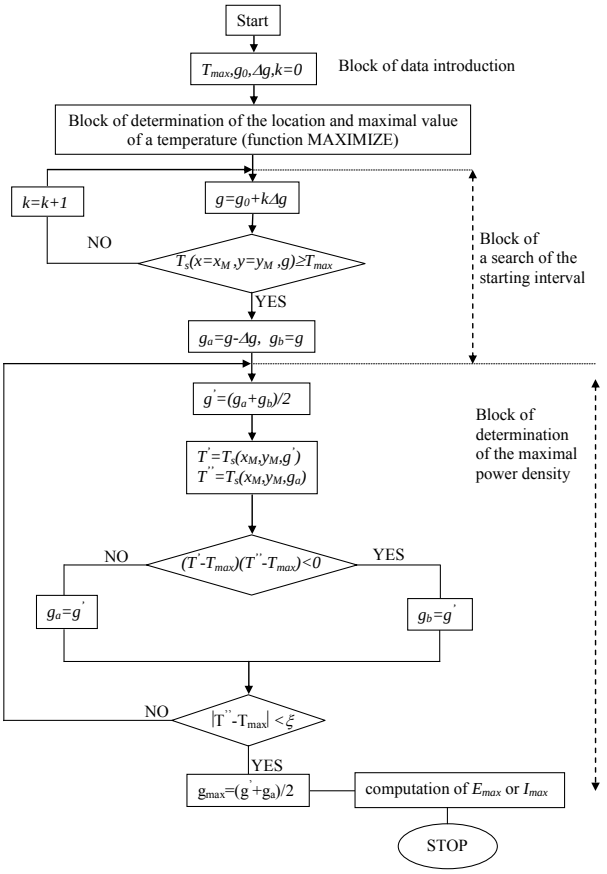

Fig. 2 Simplified block diagram of the algorithm for determination of the maximal power density

Selection of the power density conditioned by the sustained maximal temperature

Determination of the location and value of the maximal temperature is very important. Because on that basis the admissible power density g_{max} can be determined. In case of a busway it enables computation of the steady state current rating I_{max} (from (2a) after exchange $I \rightarrow I_{max}$). In turn of a dielectric charge the power density determines admissible electric field strength E_{max} (from (2b) after exchange $E \rightarrow E_{max}$). In both of the mentioned cases the temperature is a rising function of the density of a generated power. Than in order to determine maximal power density (and then I_{max} or E_{max}) it is sufficient to solve the following equation with respect to g_{max}

(11) $$T(x = x_M, y = y_M, g = g_{\max}) = T_{\max},$$

where x_M, y_M - coordinates of the point of the maximal temperature, T_{max} - sustained maximal temperature for a busway or maximal temperature of a charge limited by material and technological requirements.

In order to determine I_{max} or E_{max} the algorithm presented in Fig. 2 was developed. It was implemented on the Mathematica platform [14]. In Fig. 2 five functional blocks were shown:

I) segment of introduction of the necessary data (in dependence on the analyzed model),

II) segment of investigation of the coordinates of the warmest point:

For determination of the extremes, functions accessible in the Mathematica programme [14] were used. The MAXIMIZE[…] function was chosen based on the analytical (symbolic) method for finding maximums of the function of two variables in the given area (rectangle $\{|x| \leq a,\ 0 \leq y \leq b\}$ in case of a dielectric charge). Because of the thermal danger of surroundings, in case of a busway the domain of investigations is its perimeter $\{x=\pm a,\ y=0,\ y=b\}$. In that situation maximums of the single variable function (the other variable is a coordinate of the edge) are determined on each edge. A final location of the point of the highest temperature on a perimeter results from the comparison of maximal values determined for each side of the busway.

III) segment for finding a starting interval $<g_a, g_b>$,

IV) segment of determination of the maximal power density by the method of bisection [15] with accuracy ξ [16],

V) segment of computation of the steady state current rating I_{max} or maximal field strength E_{max}.

Computational examples

The computer programme was developed in terms of the Mathematica package [14]. It determines field distributions (10) and computes the steady state current rating I_{max} or the maximal electric field strength E_{max} (Fig. 2). Two different models were investigated. In the first case an aluminum busway was analyzed. The following data were assumed:

(12)
$a=0.005m,\ b=0.04m,\ T_o=25^oC,\ T_{max}=100^oC,\ \lambda=229W/(mK),\ \rho(T_{max}=100^oC)=4\cdot10^{-8}\Omega m,\ \xi=0.01^oC,\ \alpha_V=11.1W/(m^2K),\ \alpha_L=9W/(m^2K),\ \alpha_H=14.9W/(m^2K),\ \Delta g=500W/m^3,\ g_o=1000W/m^3.$

For the set of data (12) the following results were obtained: $x_M=\pm a,\ y_M=0.0151m,\ g_{max}=211255W/m^3$ and $I_{max}=919.2A$.

In the second case capacitative heating of a fir plank with 10% of water contain was considered. The following data were assumed:

(13)
$a=0.015m,\ b=0.1m,\ T_o=25^oC,\ T_{max}=70^oC,\ \lambda=0.13W/(mK),\ f=13.56MHz,\ \varepsilon'=3.2,\ tg\delta=0.09,\ \xi=0.01^oC,\ \alpha_V=11.1W/(m^2K),\ \alpha_L=9.7W/(m^2K),\ \alpha_H=12.9W/(m^2K),\ \Delta g=500W/m^3,\ g_o=1000W/m^3.$

For the set (13) there were determined: $x_M=0m,\ y_M=0.049m,\ g_{max}=21398.4W/m^3$ and $E_{max}=9930V/m$.

Infinite series appearing in (5a) in computation of the field distributions was found to be rapid convergent. In case of the busway, with summation of more than two terms in (5a), results didn't changed even on the eighth place after

the decimal point (independently of the choice of a point). In that conditions the summation was reduced to first three terms of (5a). In turn in case of the capacitative heating, the convergence of (5a) was slower and depended in higher degree from location of the point. The worst convergence appeared in corners of the system. Finally in the computations of a dielectric charge 30 terms of (5a) were considered. Increase of the summation index to 50 terms caused a change of the result on 4-th place after the decimal point at the given above points of the slowest convergence.

The results of computations of both models were shown in the graphic form. In Fig. 3 the field distribution was shown in a busway loaded by the steady state current rating $I_{max}=919.2A$. In turn in Fig. 4 the temperature field distribution was illustrated in a wooden plank with the maximal electric field strength $E_{max}=9930V/m$.

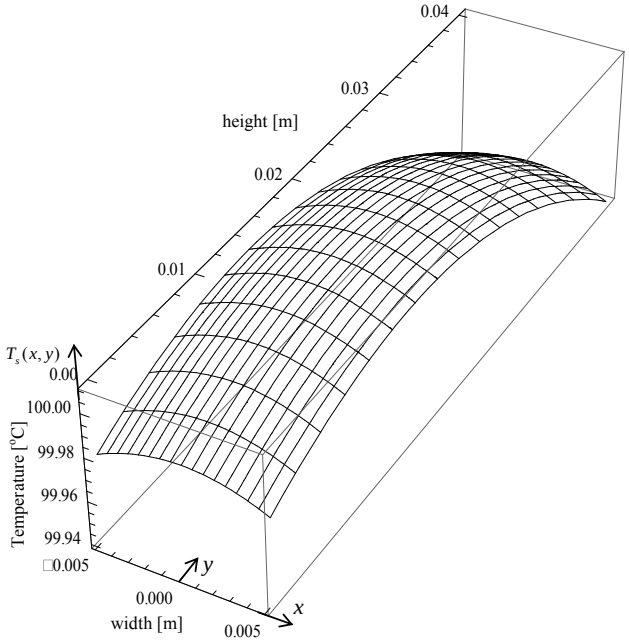

Fig. 3 Distribution of the thermal field in an aluminum busway with loading by the steady state current rating $I_{max}=919.2A$

Verification of the presented method was carried out, as well. For this aim the obtained results were compared with the computations realized by the finite element method [17]. It is a background of the NISA/HEAT TRANSFER programme [18], which was utilized in the numerical analysis. The both models were approximated by a mesh consisting of 800 quadrupole elements and 2521 nodes. In order to discretise the boundary problem (1)–(3) on the plane (x,y), the NISA v. 16 programme takes advantage of Galerkin's procedure [19]. It leads to the implicit scheme (i.e. to the matrix equation with respect to the temperature at nodes). It was solved by the iterative method [18]. This way the investigated temperature vector was determined. Then relative differences of the distributions were computed in accordance with the formula

$$100\%\frac{T_{FE}(x,y)-T_{AN}(x,y)}{T_{FE}(x,y)}, \text{ where} \tag{14}$$

$T_{AN}(x,y)$ - temperature distribution obtained by the developed analytical method, $T_{FE}(x,y)$ - temperature distribution computed by the finite element method. In Fig. 5 and Fig. 6 relation (14) was illustrated in a busway and in a wood, respectively.

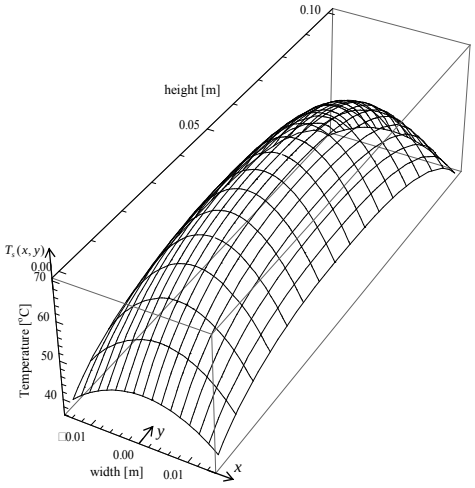

Fig. 4 Distribution of the thermal field in a fir plank (of 10% water contain) with the admissible maximal electric field strength $E_{max}=9930V/m$

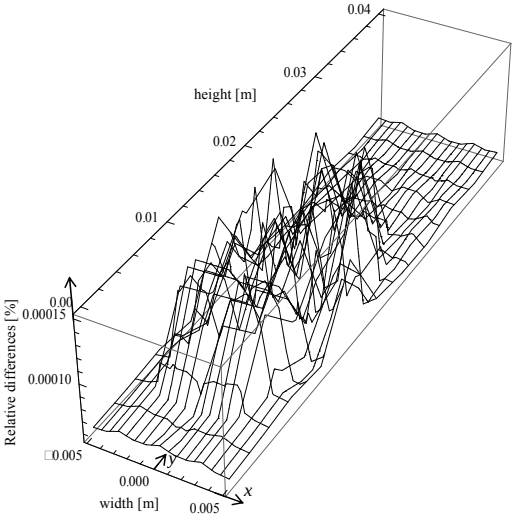

Fig. 5 Relative differences of the temperature distributions obtained in a busway by the finite element method and by the analytical one

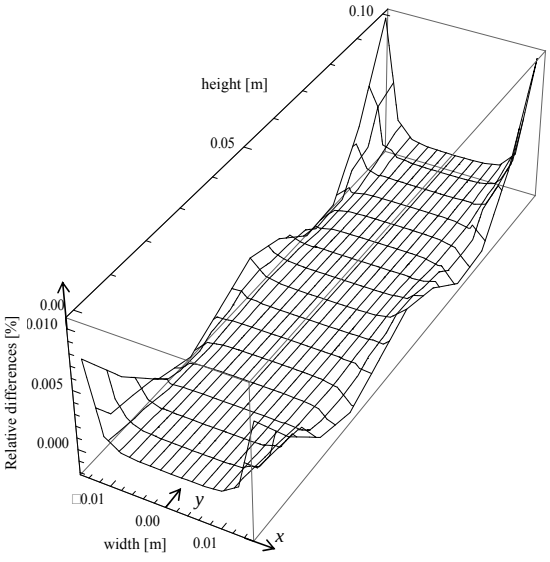

Fig. 6 Relative differences of the temperature distributions obtained in a fir plank by the finite element method and by the analytical one

Final remarks

A) From Fig. 3 follows, that the temperature distribution in a busway is almost uniform in the whole region $\{|x| \le a$, and $0 \le y \le b\}$. The difference between the maximal and minimal temperature considered in the system (not on a perimeter) is only $\Delta T=T(x=0,y=0.375b)-(x=\pm a,y=b)=0.07^oC$. The physical reason of the above phenomenon is very large the thermal conductivity of aluminum. A different picture of the field is observed in case of the capacitative heating of wood (fig. 4). Important irregularity of the field distributions was observed there. The difference between the maximal and minimal temperature in a model reached up to $\Delta T=T(x=0,y=0.49b)-T(x=\pm a,y=b)=33.6^oC$. It is caused by the relatively small value of the thermal conductivity of wood. In Fig. 3 and 4 it can be noticed, as well, that (independent of a model) a slightly higher temperature arised on the bottom edge of the system ($y=0$) than on the top one ($y=b$). The reason of that, first of all, were higher values of the heat transfer coefficients from the top edges of the models than from the bottom ones i.e. $\alpha_H > \alpha_L$.. From Fig. 3 and Fig. 4 follows, as well, that the highest temperature of both models was reached in their interior. Maximums on the plane $x=0$ are shifted with respect to the geometrical centre of the system in direction to the bottom edge ($y=0$) of the highest temperature. In Fig. 3 and Fig. 4 a symmetry can be noticed of the field distribution with respect to the plane $x=0$. It results from the same values of heat transfer coefficients from vertical walls of the models ($x=\pm a$). Then the obtained solutions have a good physical interpretation.

B) In both considered systems the relative differences of temperature distributions (computed by the finite element method and by the analytical one) are very small (Fig. 5 and Fig. 6). Because of a smaller density of the FE mesh larger deviations are observed, after all, in the case of the capacitative heating (Fig. 6). Then the presented solution (10) can be admitted as verified.

ACKNOWLEDGMENT

The article was prepared in a framework of the project S/WE/1/13 realized in the Chair of Theoretical Electrotechnic and Metrology in the Polytechnic of Bialystok.

Appendix

The proof of orthogonality of the functional sequence $\left(\frac{\alpha_L b}{\gamma_n \lambda}\sin(\gamma_n \frac{y}{b})+\cos(\gamma_n \frac{y}{b})\right)$ in a sector $\langle 0,b\rangle$.

For $n \neq m$ it takes place $I(n,m)=\int_0^b\left(\frac{\alpha_L b}{\gamma_n \lambda}\sin(\gamma_n \frac{y}{b})+\cos(\gamma_n \frac{y}{b})\right)\left(\frac{\alpha_L b}{\gamma_m \lambda}\sin(\gamma_m \frac{y}{b})+\cos(\gamma_m \frac{y}{b})\right)dy =$

$$= \frac{\alpha_L^2 b^3\left(\gamma_m \cos\gamma_m \sin\gamma_n - \gamma_n \cos\gamma_n \sin\gamma_m\right)}{\gamma_n\gamma_m\lambda^2\left(\gamma_n^2-\gamma_m^2\right)} - \frac{\alpha_L b^2\left(\gamma_n \cos\gamma_n \cos\gamma_m + \gamma_m \sin\gamma_n \sin\gamma_m - \gamma_n\right)}{\gamma_n\lambda\left(\gamma_n^2-\gamma_m^2\right)} -$$

$$- \frac{\alpha_L b^2\left(\gamma_m \cos\gamma_m \cos\gamma_n + \gamma_n \sin\gamma_m \sin\gamma_n - \gamma_m\right)}{\gamma_m\lambda\left(\gamma_m^2-\gamma_n^2\right)} + \frac{b\left(\gamma_n \sin\gamma_n \cos\gamma_m - \gamma_m \cos\gamma_n \sin\gamma_m\right)}{\left(\gamma_n^2-\gamma_m^2\right)} =$$

$$= \frac{b^2\alpha_L}{\lambda\gamma_n\gamma_m}\sin\gamma_n\sin\gamma_m - \frac{b}{\left(\gamma_m^2-\gamma_n^2\right)}\frac{(\gamma_n^2\lambda^2+\alpha_L^2b^2)}{\gamma_n\lambda^2}\cos\gamma_m\sin\gamma_n + \frac{b}{\left(\gamma_m^2-\gamma_n^2\right)}\frac{(\gamma_m^2\lambda^2+\alpha_L^2b^2)}{\gamma_m\lambda^2}\cos\gamma_n\sin\gamma_m.$$

To the above formula equation of eigenvalues (6) was substituted in the form

$\sin\gamma_n = \frac{(\alpha_L+\alpha_H)\lambda\gamma_n b}{\gamma_n^2\lambda^2-\alpha_L\alpha_H b^2}\cos\gamma_n$ and the same but with respect to the series of eigenvalues γ_m. Hence it follows, that

$$I(n,m) = \frac{b^2\alpha_L}{\lambda\gamma_n\gamma_m}\cdot\frac{(\alpha_L+\alpha_H)\lambda\gamma_n b}{\gamma_n^2\lambda^2-\alpha_L\alpha_H b^2}\cdot\frac{(\alpha_L+\alpha_H)\lambda\gamma_m b}{\gamma_m^2\lambda^2-\alpha_L\alpha_H b^2}\cos\gamma_n\cos\gamma_m - \frac{b}{\left(\gamma_m^2-\gamma_n^2\right)}\cdot\frac{\gamma_n^2\lambda^2+\alpha_L^2b^2}{\gamma_n\lambda^2}\cdot\frac{(\alpha_L+\alpha_H)\lambda\gamma_n b}{\gamma_n^2\lambda^2-\alpha_L\alpha_H b^2}\cos\gamma_n\cos\gamma_m +$$

$$+ \frac{b}{\left(\gamma_m^2-\gamma_n^2\right)}\cdot\frac{\gamma_m^2\lambda^2+\alpha_L^2b^2}{\gamma_m\lambda^2}\cdot\frac{(\alpha_L+\alpha_H)\lambda\gamma_m b}{\gamma_m^2\lambda^2-\alpha_L\alpha_H b^2}\cos\gamma_n\cos\gamma_m =$$

$$(15) \quad = \cos\gamma_n\cos\gamma_m\left(\frac{\lambda b^2\gamma_n\gamma_m(\alpha_L+\alpha_H)\left[\lambda^2b^2\alpha_L\left(\gamma_m^2-\gamma_n^2\right)(\alpha_L+\alpha_H)-\left(\gamma_m^2\lambda^2-\alpha_L\alpha_H b^2\right)\left(\gamma_n^2\lambda^2+\alpha_L^2b^2\right)+\left(\gamma_m^2\lambda^2+\alpha_L^2b^2\right)\left(\gamma_n^2\lambda^2-\alpha_L\alpha_H b^2\right)\right]}{\lambda^2\gamma_n\gamma_m\left(\gamma_m^2-\gamma_n^2\right)\left(\gamma_n^2\lambda^2-\alpha_L\alpha_H b^2\right)\left(\gamma_m^2\lambda^2-\alpha_L\alpha_H b^2\right)}\right)=0.$$

A square of the norm of the considered functional sequence has to be determined yet

$$\left\|N(m)\right\|^2 = \int_0^b\left(\frac{\alpha_L b}{\gamma_m\lambda}\sin(\gamma_m\frac{y}{b})+\cos(\gamma_m\frac{y}{b})\right)^2 dy = \frac{4b^2\lambda\alpha_L\gamma_m\sin^2\gamma_m + (b\lambda^2\gamma_m^2-b^3\alpha_L^2)\sin 2\gamma_m + 2b\lambda^2\gamma_m^3 + 2b^3\alpha_L^2\gamma_m}{4\lambda^2\gamma_m^3}.$$

After substitution of the equation of eigenvalues and respective simplification it was obtained

$$(16) \quad \left\|N(m)\right\|^2 = \frac{(b^2\alpha_L^2+\lambda^2\gamma_m^2)\left[(b^2\alpha_H\alpha_L+\lambda^2\gamma_m^2)\sin^2\gamma_m + b\lambda\gamma_m^2(\alpha_H+\alpha_L)\right]}{2\lambda^3\gamma_m^4(\alpha_H+\alpha_L)} > 0$$

Then finally from relations (15) and (16) follows, that

$$I(n,m)=\int_0^b\left(\frac{\alpha_L b}{\gamma_n\lambda}\sin(\gamma_n\frac{y}{b})+\cos(\gamma_n\frac{y}{b})\right)\left(\frac{\alpha_L b}{\gamma_m\lambda}\sin(\gamma_m\frac{y}{b})+\cos(\gamma_m\frac{y}{b})\right)dy=$$

$$=\begin{cases}0 & for\ \ n\neq m\\ \|N(m)\|^2>0 & for\ \ n=m\end{cases}$$

QED (quod erat demonstrandum).

REFERENCES

[1] Hering M., Podstawy elektrotermii. Część II, (Fundamentals of electric heating engineering. Part II), *WNT*, Warszawa (1988) (in Polish).

[2] Kulas S., Tory prądowe i układy zestykowe, (Current lines and contact systems), *Oficyna Wydawnicza Politechniki Warszawskiej*, Warszawa (2008) (in Polish).

[3] Maksymiuk J., Pochanke Z., Obliczenia i badania diagnostyczne aparatury rozdzielczej, (Computation and diagnostic investigations of power distributing apparatus), *WNT*, Warszawa (2001) (in Polish).

[4] Fleischman G. J., Predicting temperature range in food slabs undergoing long term/low power microwave heating, *Journal of Food Engineering,* 27 (1996), 337-351.

[5] Kącki E., Równania różniczkowe cząstkowe w zagadnieniach fizyki i techniki, (Partial differential equations in the problems of physics and technology), *WNT*, Warszawa (1992) (in Polish).

[6] Hering M., Termokinetyka dla elektryków, (Thermokinetics for electricians)*, WNT*, Warszawa (1980) (in Polish).

[7] Ciok Z., Metody obliczania pól elektromagnetycznych i przepływowych, (The methods of computation of the electromagnetic and flow fields), *Wydawnictwa Politechniki Warszawskiej,* Warszawa (1981) (in Polish).

[8] Turowski J., Obliczenia elektromagnetyczne elementów maszyn i urządzeń elektrycznych, (Electromagnetic computations of the elements of electrical machinery and devices), *WNT*, Warszawa (1982) (in Polish).

[9] Fleischman G. J., Predicting temperature range in food slabs undergoing short- term/high-power microwave heating, *Journal of Food Engineering* (40) 1998, 81-88.

[10] Evans L. C., Równania różniczkowe cząstkowe, (Partial differential equations), *PWN*, Warszawa (2002) (in Polish).

[11] Baehr M. D., Stephan K., Heat and mass transfer, *Springer-Verlag*, Berlin, Haidelberg (2006).

[12] Latif M. J., Heat conduction, *Springer-Verlag*, Berlin, Haidelberg (2009).

[13] Bobrowski D., Mikołajski J., Morchało J., Równania różniczkowe cząstkowe w zastosowaniach, (Partial differential equations in applications), *Wydawnictwo Politechniki Poznańskiej*, Poznań (1995) (in Polish).

[14] Grzymkowski R., Kapusta A., Kumoszek T., Słota D., Mathematica 6, *Wydawnictwa Pracowni Komputerowej Jacka Skalmierskiego*, Gliwice (2008) (in Polish).

[15] Fortuna Z., Macukow B., Wąsowski J., Metody numeryczne, (Numerical methods), *WNT*, Warszawa (1993) (in Polish).

[16] Gołębiowski J., Zaręba M., Analytical method of computation of the thermal field in a DC lead with the variable heat transfer coefficient on its surface, *Przegląd Elektrotechniczny* (88) 2012, no. 4a, 187-192.

[17] Sikora J., Numeryczne metody rozwiązywania zagadnień brzegowych, (Numerical methods for solving boundary problems), *Politechnika Lubelska*, Lublin (2011).

[18] Manuals for NISA v. 16. NISA Suite of FEA Software (CD-ROM), *Cranes Software*, Inc., Troy, MI (2008).

[19] Brenner S., Scott R. L., The mathematical theory of finite element methods, *Springer*, Berlin (2008).

***Authors**: Prof. J. Gołębiowski[1], M. Zaręba[2], Ph. D., Bialystok Technical University, Faculty of Electrical Engineering, Wiejska 45D st., 15-351 Białystok, e-mail: [1] j.golebiowski@pb.edu.pl, [2] m.zareba@pb.edu.pl*